Optica Applicata, Vol. XLIV, No. 1, 2014
DOI: 10.5277/oa140104

Design of all-optical time-division multiplexing scheme with the help of microring resonator

JAYANTA KUMAR RAKSHIT[1], JITENDRA NATH ROY[2*]

[1]Department of Electronics and Instrumentation Engineering,
National Institute of Technology, Agartala, Tripura, India

[2]Department of Physics, National Institute of Technology, Agartala, Tripura, India

[*]Corresponding author: jnroys@yahoo.co.in

Optical time-division multiplexing is a natural multiplexing technique leading to terabit/s transmission capacity for many services that will be found in near future optical telecommunication networks. In this paper we have conducted a theoretical study of all-optical time-division multiplexing switching using GaAs-AlGaAs based microring resonator together with performances characteristics. The proposed circuit is more compact, simple and will be helpful in designing all-optical telecommunication circuits in near future. Numerical simulation results confirming described methods are given in this paper.

Keywords: all-optical multiplexing, all-optical signal processing, optical logic gate, optical time-division multiplexing (OTDM), microring resonator.

1. Introduction

The growth of the Internet has led to a rush in demand for bandwidth in telecommunications networks. This trend has stimulated the rapid evolution of optical networking technologies in recent years [1, 2]. In packet routing, the optical signal entering the router is converted to an electronic signal and demultiplexed into lower-rate streams that are electronically routed in the switch core and then re-multiplexed to a high-speed electronic signal that is an output from the router on the specified optical wavelength. This optical–electronic–optical conversion leads to router congestion [3] and reduced capacity in today's networks. So to accommodate the modern broadband network, very high-speed signal processing technologies must be developed not only for transmission lines, but also for transmission nodes. The goal is to handle signal rates of more than several terabits so that enormous amounts of information including data, pictures and videos can be provided to many subscribers through optical fiber cables. So the work is underway to develop second-generation optical networks that provide continuous optical paths using optical add-drop multiplexers (OADMs). With these technologies, individual wavelength channels can be routed between nodes or switched on/off the network using all-optical techniques. The key technologies include ultrashort optical pulse generation/modulation, all-optical multiplexing/demultiplexing, optical linear or nonlinear transmission, all-optical repeating, all-optical regenerating, optical sampling, *etc*. Multiplexing and demultiplexing [4–8] are two essential features in almost all the data and signal communication and networking systems, where a lot of information is being handled without any mutual disturbances. Electronic systems are incapable of processing a large number of data at high speed (far above gigahertz). Optics is a promising candidate in this regard [9–14].

The dream of photonics is to have a completely all-optical technology. Optical nonlinear materials (ONLM) provide a major support to optical switching based all-optical logic and algebraic processing [15–28]. In this paper we have tried to exploit the advantages of special nonlinear characteristics of a ring resonator [29–36] for designing time-division multiplexing schemes which will work in all-optical domain [37–38]. The proposed all-optical multiplexer can exhibit its switching speed far above present day electronic switches. The proposed circuit is simpler and less complex rather than the reference one [39] and better suited for an integrated circuit design. The optical time multiplexing scheme using an optical coupler and optical delay line has been reported [40], where the circuit is serial in nature. In that paper, ZHAN-QIANG HUI and JIAN-GUO ZHANG modulated the optical data signal with a return to zero (RZ) pseudo-random binary sequence (PRBS) and had sent it to the input of the multiplexer serially. But the advantage of our paper is that the proposed structure is parallel in nature. All the optical data inputs can be given simultaneously and according to the select inputs, any one of the given data can be transferred to the output. On the other hand, the design reported in reference [40] has used 1×2, 2×2, 2×1 couplers and optical delay lines. So higher order optical time-division multiplexing (OTDM) design is quite difficult as the input power of the optical couplers is divided into two parts.

The main advantages/novelties of the proposed model represented in this paper are:

– The proposed circuit is all-optical in nature.

– The proposed OTDM circuit is designed using only microring resonators and the circuit is very attractive due to its (microring resonator) intrinsic advantages like compactness and reduced power consumption.

– Another potential advantage of OTDM circuit using the microring resonator is the possible simplification of network management and versatile implementation of network functionalities for enhanced signal processing applications.

– The proposed model can easily be extended for higher order inputs due to simple circuitry. No major modification and no other components rather than ring resonator is needed in designing the circuit.

The paper is organized as follows: Operational principle of all-optical switches using the microring resonator is discussed in Section 2. In Section 3, the theory, design and simulation results and discussion of the proposed scheme for time-division multiplexing are explained and Section 4 is a conclusion of the paper.

2. Microring resonator based optical switch

The GaAs-AlGaAs based microring resonator consists of unidirectional coupling between a ring resonator and input-output waveguides. Parameters k_1 and k_2 are the coupling coefficient between the input waveguide and the ring and the ring and the output waveguide, respectively. A fraction k_1 of the incoming field is transferred to the ring having radius r as shown in Fig. 1**a**. When the optical path-length of a roundtrip is the integer multiple of the effective wavelength, the microring resonator will have "ON resonance" (*i.e.*, a constructive interference will occur). At resonance, the drop port shows maximum transmission and through the port shows a minimum transmittance. A logic switch can be produced if the resonator is made of a nonlinear material. Through nonlinear property of the material, the refractive index can be changed by the intensity of light in the resonator. A green laser ($\lambda = 532$ nm) is used to pump the ring from top of the ring [41] as shown in Fig. 1**b**. The high density carriers are generated (pumping introduces extra electron–hole pair) as the optical pump pulse is almost fully absorbed in the microring waveguide. These carriers effectively result in a net decrease of the refractive index of the microring waveguide and cause a temporarily blue shift of the microring resonance wavelength [42]. Hence the microring resonator acts as an optical switch and the status of the switch is controlled by the optical pump pulse.

Let us consider: E_{i1} and E_{i2} are the input and add port field, respectively, and E_t and E_d are the through port and drop port field, respectively, as shown in Fig. 1**a**.

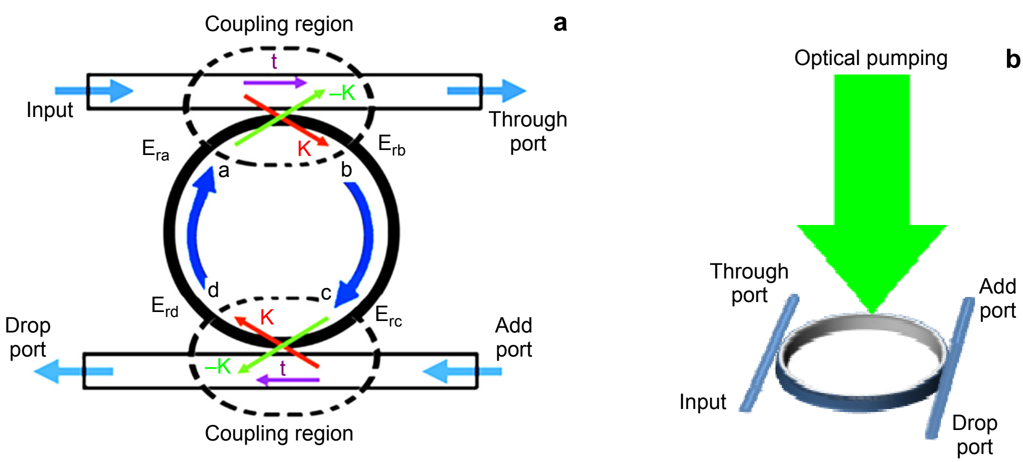

Fig. 1. Single ring resonator (**a**) and optical pumping process (**b**).

The fields at the points a, b, c and d are E_{ra}, E_{rb}, E_{rc} and E_{rd}, respectively. Then we can write [43–46]

$$E_{ra} = (1-\gamma)^{1/2}\left[j\sqrt{k_1}\,E_{i1} + \sqrt{1-k_1}\,E_{rd}\right] \tag{1}$$

$$E_{rb} = E_{ra}\exp\left(-\alpha\frac{L}{4}\right)\exp\left(jk_n\frac{L}{2}\right) \tag{2}$$

$$E_{rc} = (1-\gamma)^{1/2}\left[j\sqrt{k_2}\,E_{i2} + \sqrt{1-k_2}\,E_{rb}\right] \tag{3}$$

$$E_{rd} = E_{rc}\exp\left(-\alpha\frac{L}{4}\right)\exp\left(jk_n\frac{L}{2}\right) \tag{4}$$

where, $L = 2\pi r$ is the circumference of the ring, α is the intensity attenuation coefficient of the ring, γ is the intensity insertion loss coefficient of the directional coupler, $k_n = 2\pi n_{\mathrm{eff}}/\lambda$ is the wave propagation constant, λ is the resonant wavelength of the ring, $n_{\mathrm{eff}} = n_0 + n_2 I = n_0 + n_2 P/A_{\mathrm{eff}}$ is the effective refractive index, where n_0 and n_2 are the linear and nonlinear refractive indexes, respectively, I and P are the intensity and power of the optical pump signal, A_{eff} is the effective cross-sectional area of the ring resonator.

The fields at the through port and drop port can be written as [43–46]

$$E_t = (1-\gamma)^{1/2}\left[\sqrt{1-k_1}\,E_{i1} + j\sqrt{k_1}\,E_{rd}\right] \tag{5}$$

$$E_d = (1-\gamma)^{1/2}\left[\sqrt{1-k_2}\,E_{i2} + j\sqrt{k_2}\,E_{rb}\right] \tag{6}$$

Equations (5) and (6) can also be expressed as follows (detail calculation is given in Appendix)

$$E_t = \frac{D\sqrt{1-k_1} - D\sqrt{1-k_2}\,x^2\exp^2(j\varphi)}{1-\sqrt{1-k_1}\sqrt{1-k_2}\,x^2\exp^2(j\varphi)}E_{i1} + \frac{-D\sqrt{k_1}\sqrt{k_2}\,x\exp(j\varphi)}{1-\sqrt{1-k_1}\sqrt{1-k_2}\,x^2\exp^2(j\varphi)}E_{i2} \tag{7}$$

$$E_d = \frac{-D\sqrt{k_1}\sqrt{k_2}\,x\exp(j\varphi)}{1-\sqrt{1-k_1}\sqrt{1-k_2}\,x^2\exp^2(j\varphi)}E_{i1} + \frac{D\sqrt{1-k_2} - D\sqrt{1-k_1}\,x^2\exp^2(j\varphi)}{1-\sqrt{1-k_1}\sqrt{1-k_2}\,x^2\exp^2(j\varphi)}E_{i2} \tag{8}$$

where $D = (1-\gamma)^{1/2}$, $x = D\exp(-\alpha L/4)$ and $\varphi = k_n L/2$.

The above equations help to design a ring resonator as a switch and the above nonlinear characteristics of the microring resonator is utilized for designing a reverse tree-net architecture in all-optical domain which can successfully be exploited for time-division all-optical data multiplexing scheme.

3. Designing of time-division multiplexing scheme

3.1. Theoretical model

Multiplexer or data selector is a logic circuit that accepts several data inputs and allows only one of them at a time to go to the output. The routing of the desired data input to the output is controlled by select (control) inputs. Figure 2 shows the functional diagram of a general multiplexer where normally there are 2^n input lines and n select lines whose bit combination determines which input is to be selected.

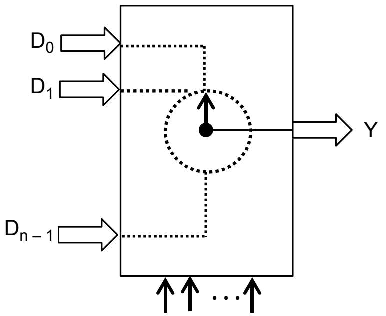

◄ Fig. 2. Block diagram of a multiplexer.

In our proposed all-optical 4×1 multiplexing scheme, D_0, D_1, D_2, and D_3 are the input data signals, A and B are the control signals and Y is the output signal. Switching property of the microring resonator (MRR), discussed above in Section 2, can be exploited successfully for designing an all-optical multiplexing scheme. Figure 3 shows the architecture for designing all-optical 4×1 multiplexing schemes where the output is taken from the drop port of the MRR3. Figure 4 shows the proposed experimental setup of an all-optical 4 ×1 multiplexing scheme.

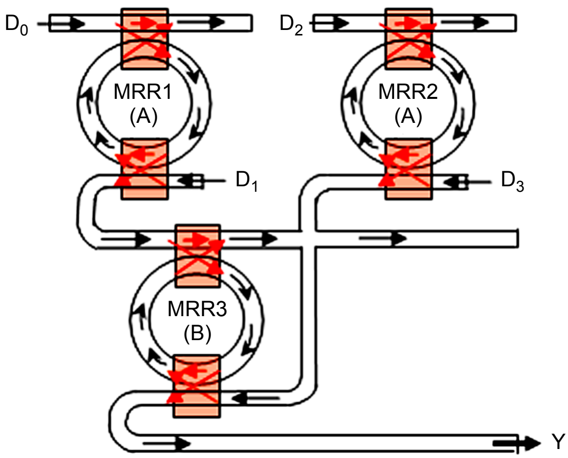

Fig. 3. All-optical 4×1 multiplexing scheme.

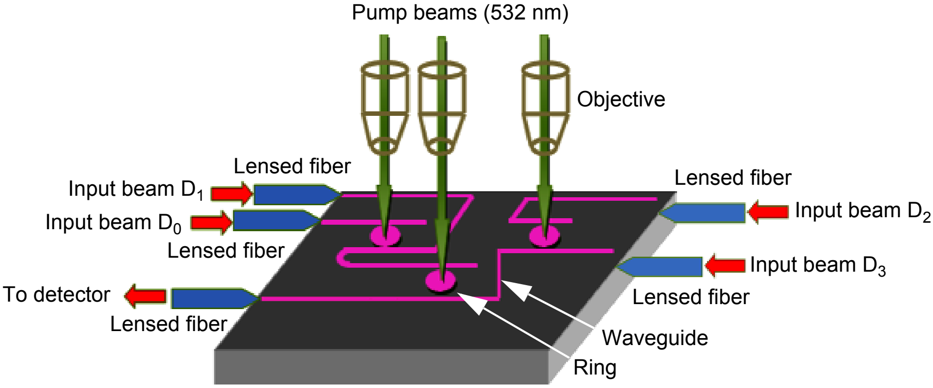

Fig. 4. Proposed experimental setup of an all-optical 4×1 multiplexing scheme.

The logic levels applied to the A and B control inputs (pump signals) determine which port of the rings is enabled, so that its data input passes through the ring to the output. The expression for the output is given by:

$$Y = \bar{A}\bar{B}D_0 + \bar{A}BD_1 + A\bar{B}D_2 + ABD_3 \tag{9}$$

3.2. Simulation result

In simulation, the parameters [30, 46–48] used for GaAs-AlGaAs microring resonator are summarized in Table 1.

The operational principle is discussed for different possible combinations, and computer simulated results (using MATLAB 7.6) are reported in Fig. 5. Result is also given in a tabular form as shown in Table 2.

Case 1 (when $A = B = 0$). When $A = 0$ and $B = 0$ (*i.e.*, no pump signal is applied to the rings), input data signals D_0 and D_2 will appear at the drop port of MRR1 and MRR2 which act as the input port and add port of MRR3, respectively. As $B = 0$, the input port signal D_0 will appear at the drop port of MRR3 which is the desired output. This

Table 1. Parameters and their optimum values used in simulation.

Parameters	Optimized value
Coupling coefficient for MRR1	0.25
Coupling coefficient for MRR2	0.25
Coupling coefficient for MRR3	0.25
Resonant wavelength	1.55 μm
Radius of the ring	7.08 μm
Effective cross-sectional area	0.25 μm^2
Resonant wavelength with pumping power	1.5485 μm
Change of refractive index when pumping power applied	3×10^{-3}
Intensity attenuation coefficient of the ring	0.0005 μm^{-1}

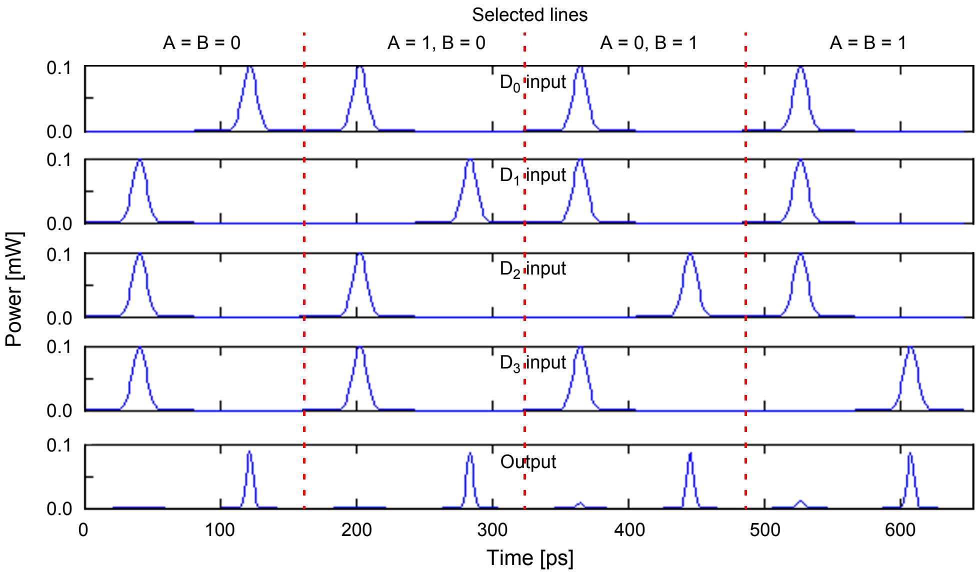

Fig. 5. Simulation output of 4×1 multiplexer.

T a b l e 2. The truth table of 4×1 multiplexer (X – "don't care").

Control (select) inputs		Data inputs				Output Y	
A	B	D_0	D_1	D_2	D_3		
0	0	0	X	X	X	0	D_0
0	0	1	X	X	X	1	
1	0	X	0	X	X	0	D_1
1	0	X	1	X	X	1	
0	1	X	X	0	X	0	D_2
0	1	X	X	1	X	1	
1	1	X	X	X	0	0	D_3
1	1	X	X	X	1	1	

shows that the input data signal D_0 can be sent to the output terminal Y when control signals are $A = 0$ and $B = 0$.

Case 2 (when $A = 1$, $B = 0$). When first control pump signal A is on state and second control pump signal B is off state, input data signals D_1 and D_3 will appear at the drop ports of MRR1 and MRR2 which act as the input port and add port of MRR3, respectively. As $B = 0$, the input port signal D_1 will appear at the drop port of MRR3 which is the desired output. This shows that the input data signal D_1 can be sent to the output Y keeping control signals $A = 1$ and $B = 0$.

Case 3 (when $A = 0$, $B = 1$). When first control pump signal A is off state and second control pump signal B is on state, input data signals D_0 and D_2 will again appear at the drop ports of MRR1 and MRR2 which act as the input port and add port of MRR3, respectively. But as $B = 1$, the add port signal D_2 will appear at the drop port of MRR3 which is the desired output. This shows that the input data signal D_2 can be sent to the output Y keeping control signals $A = 0$ and $B = 1$.

Case 4 (when $A = B = 1$). When both control pump signals (A and B) are on state, input data signals D_1 and D_3 will again appear at the drop ports of MRR1 and MRR2 which act as the input and add port of MRR3, respectively. But as $B = 1$, the add port signal D_3 will appear at the drop port of MRR3 which is the desired output. This shows that the input data signal D_3 can be sent to the output Y keeping control signals $A = B = 1$.

All the eight possible combinations as shown in simulation results are shown in Table 2.

3.3. Discussion

To measure the performance of the proposed circuit, we define and calculate different "figure of merits" from the simulation output, such as the on-off ratio, extinction ratio, contrast ratio and amplitude modulation [49–52].

One important parameter of the microring resonator based multiplexer circuit is the on-off ratio which is the ratio of the on-resonance intensity to the off-resonance intensity which is given by

$$\text{ON-OFF ratio} = \frac{T_{\text{max(through port)}}}{T_{\text{min(drop port)}}} \tag{10}$$

High performance microring resonator based multiplexer circuit can be realized using the high on-off ratio >20 dB and the calculated value from the simulation is nearly 25 dB.

Output signal is switched on and off by the input pulses and control pulse, showing ultrafast rising and falling edges. When input = 1 and control = 1, the signal starts to rise and when input = 0, control = 1, the signal goes to a low level. The rise time and falling time for the proposed model is shown in Figs. 6**a** and 6**b**, respectively. From the figures, we have calculated switching speed of 4 ps for rise time and 3.8 ps for falling time.

High extinction ratio (ER) makes the ultrafast all-optical multiplexer suitable to be exploited to control all-optical switch. The high value of extinction ratio distinguishes the high (1) to the low (0) level very clearly.

$$\text{ER (dB)} = 10\log\left(\frac{P^1_{\text{min}}}{P^0_{\text{max}}}\right) \tag{11}$$

where P^1_{min} and P^0_{max} are the minimum and maximum values of the peak intensity of the high (1) and low (0) level, respectively. The dependence of the output ER on the coupling coefficient is shown in Fig. 7. To find the optimum value of ER, we

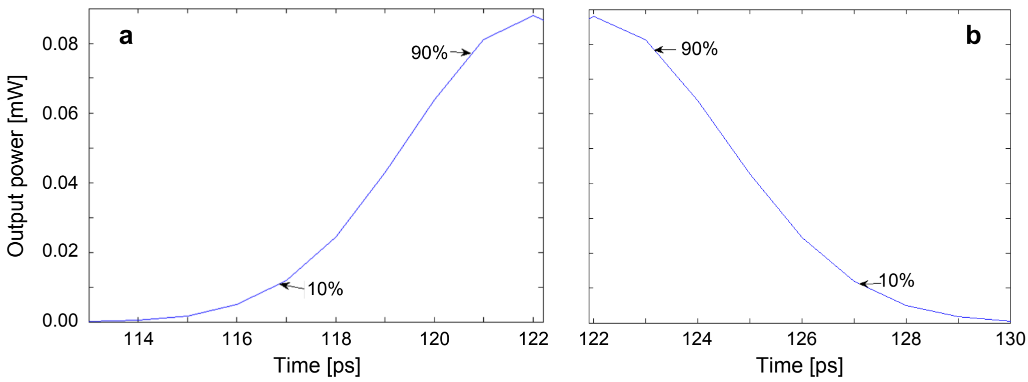

Fig. 6. Switching speed for rise (**a**) and falling (**b**) time.

change the coupling coefficient of the MRR3 of the proposed scheme. The graph shows that the ER becomes maximum (20.8 dB) at 0.2 coupling coefficient which is our desired value.

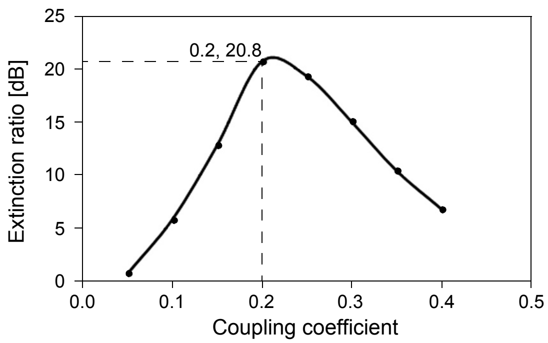

Fig. 7. Extinction ratio against coupling coefficient.

The output contrast ratio (CR) is defined as the ratio of the mean value of output intensity for 1 (P^1_{mean}) to the mean output intensity for 0 (P^0_{mean}) and given as

$$\mathrm{CR\ (dB)} = 10 \log\left(\frac{P^1_{\mathrm{mean}}}{P^0_{\mathrm{mean}}}\right) \tag{12}$$

For optimum performance the CR must be as high as possible so that the main fraction of the input can exist at the output. The dependence of the output CR on the coupling coefficient is shown in Fig. 8. To find the optimum value of CR, we change the coupling coefficient of the MRR3 of the proposed scheme. The graph shows that the CR becomes maximum (20.1 dB) at 0.2 coupling coefficient which is our desired value.

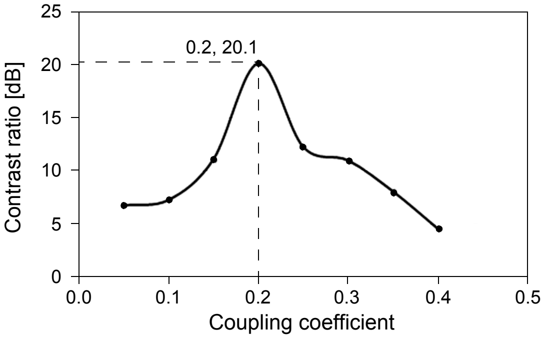

Fig. 8. Contrast ratio against coupling coefficient.

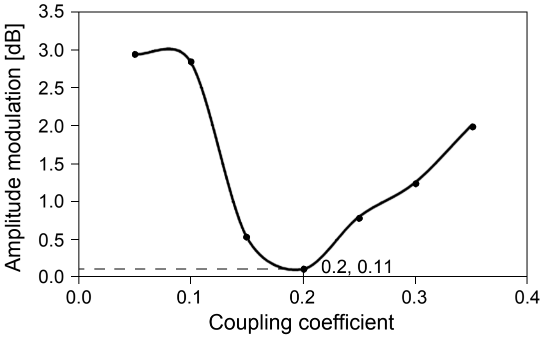

Fig. 9. Amplitude modulation against coupling coefficient.

The amplitude modulation (AM) can be defined as

$$\mathrm{AM\ (dB)} = 10 \log\left(\frac{P^1_{\max}}{P^1_{\min}}\right) \tag{13}$$

where $P^1_{\max}$ and $P^1_{\min}$ are the maximum and minimum value of intensity at the high (1) level. Typically, this metric must be lower than 1 dB [53]. The dependence of the output AM on the coupling coefficient is shown in Fig. 9. To find the optimum value of AM, we change the coupling coefficient of the MRR3 of the proposed scheme. The graph shows that the AM becomes minimum (0.11 dB) at 0.2 coupling coefficient which is our desired value.

4. Conclusion

In conclusion we can say that applying the proper control signals, one can send any desired input data to the output channel. In this paper, we present ultrafast optical time-division multiplexed networks as a feasible means of achieving a highly capable next-generation all-optical packet-switched network which provides simple network management and self-routing of packets. Here, we have exploited the reverse tree net architecture for designing a time-division multiplexing scheme. Basically, the proposed multiplexer is very much suitable in all-optical digital signal communication. The proposed scheme can easily and successfully be extended and implemented for higher order (8×1, 16×1, 32×1 and so on) multiplexing scheme. This can be done by proper incorporation of ring resonator based optical switches, extending the reverse tree and by suitable branch selection using a control signal. Also it has been pointed out in the paper that the successful ultrahigh speed transmission is attributed to the newly developed all-optical signal processing techniques and they are expected to play important roles in constructing future all-optical photonic networks in the 21st century.

Appendix – Calculation of through port and drop port output fields of microring resonator

The field E_{ra}, E_{rb}, E_{rc}, E_{rd} can be written as (see Fig. 1**a**)

$$E_{ra} = (1-\gamma)^{1/2}\left[j\sqrt{k_1}\,E_{i1} + \sqrt{1-k_1}\,E_{rd}\right] \tag{A1}$$

$$E_{rb} = E_{ra}\exp\left(-\alpha\frac{L}{4}\right)\exp\left(jk_n\frac{L}{2}\right) \tag{A2}$$

$$E_{rc} = (1-\gamma)^{1/2}\left[j\sqrt{k_2}\,E_{i2} + \sqrt{1-k_2}\,E_{rb}\right] \tag{A3}$$

$$E_{rd} = E_{rc}\exp\left(-\alpha\frac{L}{4}\right)\exp\left(jk_n\frac{L}{2}\right) \tag{A4}$$

where $k_n = 2\pi n_{\mathrm{eff}}/\lambda$ is the wave propagation constant, λ is the resonant wavelength of the ring, $n_{\mathrm{eff}} = n_0 + n_2 I = n_0 + n_2 P/A_{\mathrm{eff}}$ is the effective refractive index, where n_0 and n_2 are the linear and nonlinear refractive indexes, respectively, I and P are the intensity and power of the optical pump signal, A_{eff} is the effective cross-sectional area of the ring resonator.

The fields at the through and drop port can be written as [38–41]

$$E_t = (1-\gamma)^{1/2}\left[\sqrt{1-k_1}\,E_{i1} + j\sqrt{k_1}\,E_{rd}\right] \tag{A5}$$

$$E_d = (1-\gamma)^{1/2}\left[\sqrt{1-k_2}\,E_{i2} + j\sqrt{k_2}\,E_{rb}\right] \tag{A6}$$

Putting the value of E_{rd} from Eq. (A4) in Eq. (A1), we get

$$E_{ra} = jD\sqrt{k_1}\,E_{i1} + \sqrt{1-k_1}\,x\exp(j\varphi)E_{rc} \tag{A7}$$

where $D = (1-\gamma)^{1/2}$, $x = D\exp(-\alpha L/4)$ and $\varphi = k_n L/2$.

Similarly putting the value of E_{rb} from Eq. (A2) in Eq. (A3), we get

$$E_{rc} = jD\sqrt{k_2}\,E_{i2} + \sqrt{1-k_2}\,x\exp(j\varphi)E_{ra} \tag{A8}$$

Putting the value of E_{rc} from Eq. (A8) in Eq. (A7), we get

$$E_{ra} = jD\sqrt{k_1}\,E_{i1} + \sqrt{1-k_1}\,x\exp(j\varphi)\left[jD\sqrt{k_2}\,E_{i2} + \sqrt{1-k_2}\,x\exp(j\varphi)E_{ra}\right] =$$

$$= \frac{jD\sqrt{k_1}\,E_{i1} + jD\sqrt{k_2}\,\sqrt{1-k_1}\,x\exp(j\varphi)E_{i2}}{1-\sqrt{1-k_1}\,\sqrt{1-k_2}\,x^2\exp^2(j\varphi)} \tag{A9}$$

Similarly putting the value of E_{ra} from Eq. (A7) in Eq. (A8), we get

$$E_{rc} = jD\sqrt{k_2}\,E_{i2} + \sqrt{1-k_2}\,x\exp(j\varphi)\left[jD\sqrt{k_1}\,E_{i1} + \sqrt{1-k_1}\,x\exp(j\varphi)E_{rc}\right] =$$

$$= \frac{jD\sqrt{k_2}\,E_{i2} + jD\sqrt{k_1}\,\sqrt{1-k_2}\,x\exp(j\varphi)E_{i1}}{1-\sqrt{1-k_1}\,\sqrt{1-k_2}\,x^2\exp^2(j\varphi)} \tag{A10}$$

Using Equation (A4), Eq. (A5) can be written as

$$E_t = D\sqrt{1-k_1}\,E_{i1} + j\sqrt{k_1}\,x\exp(j\varphi)E_{rc} \tag{A11}$$

Putting the value of E_{rc} from Eq. (A10) into Eq. (A11), we have

$$E_t = D\sqrt{1-k_1}\,E_{i1} +$$

$$+ j\sqrt{k_1}\,x\exp(j\varphi)\frac{jD\sqrt{k_2}\,E_{i2} + jD\sqrt{k_1}\,\sqrt{1-k_2}\,x\exp(j\varphi)E_{i1}}{1-\sqrt{1-k_1}\,\sqrt{1-k_2}\,x^2\exp^2(j\varphi)} =$$

$$= D\sqrt{1-k_1}\,E_{i1} + \frac{-Dk_1\sqrt{1-k_1}\,x^2\exp^2(j\varphi)}{1-\sqrt{1-k_1}\,\sqrt{1-k_2}\,x^2\exp^2(j\varphi)}E_{i1} +$$

$$+ \frac{-D\sqrt{k_1}\,\sqrt{k_2}\,x\exp(j\varphi)}{1-\sqrt{1-k_1}\,\sqrt{1-k_2}\,x^2\exp^2(j\varphi)}E_{i2} =$$

$$= \frac{D\sqrt{1-k_1} - D\sqrt{1-k_2}\,x^2\exp^2(j\varphi)}{1-\sqrt{1-k_1}\,\sqrt{1-k_2}\,x^2\exp^2(j\varphi)}E_{i1} +$$

$$+ \frac{-D\sqrt{k_1}\,\sqrt{k_2}\,x\exp(j\varphi)}{1-\sqrt{1-k_1}\,\sqrt{1-k_2}\,x^2\exp^2(j\varphi)}E_{i2} \tag{A12}$$

Using Equation (A2), Eq. (A6) can be written as

$$E_d = D\sqrt{1-k_2}\,E_{i2} + j\sqrt{k_2}\,x\exp(j\varphi)E_{ra} \tag{A13}$$

Putting the value of E_{ra} from Eq. (A9) into Eq. (A13), we have

$$\begin{aligned}
E_d &= D\sqrt{1-k_2}\,E_{i2} + \\
&\quad + j\sqrt{k_2}\,x\exp(j\varphi)\frac{jD\sqrt{k_1}\,E_{i1} + jD\sqrt{k_2}\sqrt{1-k_1}\,x\exp(j\varphi)E_{i2}}{1-\sqrt{1-k_1}\sqrt{1-k_2}\,x^2\exp^2(j\varphi)} = \\
&= D\sqrt{1-k_2}\,E_{i2} + \frac{-Dk_2\sqrt{1-k_1}\,x^2\exp^2(j\varphi)}{1-\sqrt{1-k_1}\sqrt{1-k_2}\,x^2\exp^2(j\varphi)}E_{i2} + \\
&\quad + \frac{-D\sqrt{k_1}\sqrt{k_2}\,x\exp(j\varphi)}{1-\sqrt{1-k_1}\sqrt{1-k_2}\,x^2\exp^2(j\varphi)}E_{i1} = \\
&= \frac{-D\sqrt{k_1}\sqrt{k_2}\,x\exp(j\varphi)}{1-\sqrt{1-k_1}\sqrt{1-k_2}\,x^2\exp^2(j\varphi)}E_{i1} + \\
&\quad + \frac{D\sqrt{1-k_2} - D\sqrt{1-k_1}\,x^2\exp^2(j\varphi)}{1-\sqrt{1-k_1}\sqrt{1-k_2}\,x^2\exp^2(j\varphi)}E_{i2}
\end{aligned} \tag{A14}$$

So E_t and E_d are the through port and drop port fields of the ring resonator.

Acknowledgements – Authors gratefully acknowledge the suggestions given by Tanay Chattapadhyay regarding the switching operation of a microring resonator.

References

[1] FUKUCHI K., KASAMATSU T., MORIE M., OHHIRA R., ITO T., SEKIYA K., OGASAHARA D., ONO T., *10.92-Tb/s (273×40-Gb/s) triple-band/ultra-dense WDM optical-repeatered transmission experiment*, [In] *Optical Fiber Communication Conference – Postdeadline*, Anaheim, California, March 17, 2001, article PD24.

[2] BIGO S., FRIGNAC Y., CHARLET G., IDLER W., BORNE S., GROSS H., DISCHLER R., POEHLMANN W., TRAN P., SIMONNEAU C., BAYART D., VEITH G., JOURDAN A., HAMAIDE J.-P., *10.2 Tbit/s (256×42.7 Gbit/s PDM/WDM) transmission over 100 km TeraLight™ fiber with 1.28 bit/s/Hz spectral efficiency*, [In] *Optical Fiber Communication Conference – Postdeadline*, Anaheim, California, March 17, 2001, article PD25.

[3] GLESK I., SOLOKOFF J.P., PRUCNAL P.R., *All-optical address recognition and self-routing in a 250 Gbit/s packet-switched network*, Electronics Letters **30**(16), 1994, pp. 1322–1323.

[4] YANQIAO XIE, SHIMING GAO, SAILING HE, *Simultaneous all-optical, error-free time-division demultiplexing and NRZ-to-RZ format conversion using a silicon-on-insulator waveguide*, 17th Opto-Electronics and Communications Conference (OECC), July 2–6, 2012, pp. 241–242.

[5] KUROSU T., TANIZAWA K., NAMIKI S., *Clock distribution scheme using signal phase for channel identification in optical time division multiplexing*, [In] *Optical Fiber Communication Conference*, Los Angeles, California United States, March 4–8, 2012, article OW1I.6.

[6] IBRAHIM T.A., VAN V., HO P.-T., *All-optical time-division demultiplexing and spatial pulse routing with a GaAs/AlGaAs microring resonator*, Optics Letters **27**(10), 2002, pp. 803–805.

[7] ZHAN-QIANG HUI, JIAN-GUO ZHANG, *Wavelength conversion, time demultiplexing and multicasting based on cross-phase modulation and four-wave mixing in dispersion-flattened highly nonlinear photonic crystal fiber*, Journal of Optics **14**(5), 2012, article 055402.

[8] ZHAN-QIANG HUI, JIAN-GUO ZHANG, JIA-MIN GONG, MENG LIANG, MEI-ZHI ZHANG, YI YANG, FENG-TAO HE, JI-HONG LIU, *Demonstration of 40 Gbit/s all-optical return-to-zero to nonreturn-to-zero format conversion with wavelength conversion and dual-channel multicasting based on multiple cross-phase modulation in a highly nonlinear fiber*, Optical Engineering **52**(5), 2013, article 055002.

[9] MITCHELL M., SEGEV M., *Self-trapping of incoherent white light*, Nature **387**, 1997, pp. 880–883.

[10] KARIM M.A., AWAL A.A.S., *Optical Computing: An Introduction*, Wiley, New York, 2003.

[11] GUOQIANG LI, LIREN LIU, LAN SHAO, YAOZU YIN, JIAWEN HUA, *Parallel optical negabinary arithmetic based on logic operations*, Applied Optics **36**(5), 1997, pp. 1011–1016.

[12] ROY J.N., MUKHOPADHYAY S., *A minimization scheme of optical space-variant logical operations in a combinational architecture*, Optics Communications **119**(5–6), 1995, pp. 499–504.

[13] GAYEN D.K., ROY J.N., PAL R.K., *All-optical carry lookahead adder with the help of terahertz optical asymmetric demultiplexer*, Optik – International Journal for Light and Electron Optics **123**(1), 2012, pp. 40–45.

[14] SMITH S.D., JANOSSY I., MACKENZIE H.A., MATHEW J.G., REID J.J., TAGHIZADEH M.R., TOOLEY F.A., WALKER A.C., *Nonlinear optical circuit elements as logic gates for optical computers: the first digital optical circuits*, Optical Engineering **24**(4), 1985, pp. 569–573.

[15] GAYEN D.K., BHATTACHRYYA A., CHATTOPADHYAY T., ROY J.N., *Ultrafast all-optical half adder using quantum-dot semiconductor optical amplifier-based Mach–Zehnder interferometer*, Journal of Lightwave Technology **30**(21), 2012, pp. 3387–3393.

[16] GAYEN D.K., CHATTOPADHYAY T., PAL R.K., ROY J.N., *All-optical prefix tree adder with the help of terahertz optical asymmetric demultiplexer*, Chinese Optics Letters **9**(6), 2011, article 062001.

[17] ROY J.N., GAYEN D.K., *Integrated all-optical logic and arithmetic operations with the help of a TOAD-based interferometer device – alternative approach*, Applied Optics **46**(22), 2007, pp. 5304–5310.

[18] CHERRI A.K., *Terahertz-optical-asymmetric-demultiplexer (TOAD)-based arithmetic units for ultra-fast optical information processing*, Proceedings of SPIE **7671**, 2010, article 76710N.

[19] ROY J.N., RAKSHIT J.K., *Design of micro-ring resonator-based all-optical logic shifter*, Optics Communications **312**, 2014, pp. 73–79.

[20] KARIM M.A., AWWAL A.A.S., CHERRI A.K., *Polarization-encoded optical shadow-casting logic units: design*, Applied Optics **26**(14), 1987, pp. 2720–2725.

[21] ALAM M.S., KARIM M.A., *Real-time optical arithmetic/logical processing*, Journal of Parallel and Distributed Computing **17**(3), 1993, pp. 251–258.

[22] SHUQUN ZHANG, KARIM M.A., *A new impulse detector for switching median filters*, IEEE Signal Processing Letters **9**(11), 2002, pp. 360–363.

[23] CHATTOPADHYAY T., ROY J.N., *Design of SOA-MZI based all-optical programmable logic device (PLD)*, Optics Communications **283**(12), 2010, pp. 2506–2517.

[24] GUOQIANG LI, FENG QIAN, HAO RUAN, LIREN LIU, *Compact parallel optical modified-signed-digit arithmetic-logic array processor with electron-trapping device*, Applied Optics **38**(23), 1999, pp. 5039–5045.

[25] HONGJIAN WANG, KAI SONG, *Simulative method for the optical processor reconfiguration on a dynamically reconfigurable optical platform*, Applied Optics **51**(2), 2012, pp. 167–175.

[26] GAYEN D.K., ROY J.N., *All-optical arithmetic unit with the help of terahertz-optical-asymmetric-demultiplexer-based tree architecture*, Applied Optics **47**(7), 2008, pp. 933–943.

[27] ROY J.N., MAITY G.K., GAYEN D.K., CHATTOPADHYAY T., *Terahertz optical asymmetric demultiplexer based tree-net architecture for all-optical conversion scheme from binary to its other 2*n *radix based form*, Chinese Optics Letters **6**(7), 2008, pp. 536–540.

[28] ROY J.N., *Mach–Zehnder interferometer-based tree architecture for all-optical logic and arithmetic operations*, Optik – International Journal for Light and Electron Optics **120**(7), 2009, pp. 318–324.

[29] VAN V., IBRAHIM T.A., RITTER K., ABSIL P.P., JOHNSON F.G., GROVER R., GOLDHAR J., HO P.-T., *All optical nonlinear switching in GaAs–AlGaAs microring resonators*, IEEE Photonics Technology Letters **14**(1), 2002, pp. 74–76.

[30] RAKSHIT J.K., ROY J.N., CHATTOPADHYAY T., *Design of micro-ring resonator based all-optical parity generator and checker circuit*, Optics Communications **303**, 2013, pp. 30–37.

[31] RAKSHIT J.K., CHATTOPADHYAY T., ROY J.N., *All-optical clocked D flip flop using single micro-ring resonator*, International Conference on Fiber Optics and Photonics, 2012, article WPo.29.

[32] LINSEN LI, JUNQIANG SUN, *Theoretical investigation of phase-based all-optical logic gates based on AlGaAs microring resonators*, Journal of Modern Optics **59**(13), 2012, pp. 1149–1153.

[33] HEEBNER J.E., BOYD R.W., *Enhanced all-optical switching by use of a nonlinear fiber ring resonator*, Optics Letters **24**(12), 1999, pp. 847–849.

[34] LINSEN LI, JUNQIANG SUN, *Theoretical investigation of phase-based all-optical NOT, XOR and XNOR logic gates based on AlGaAs microring resonators*, Journal of Modern Optics **59**(9), 2012, pp. 809–813.

[35] LEI ZHANG, JIANFENG DING, YONGHUI TIAN, RUIQIANG JI, LIN YANG, HONGTAO CHEN, PING ZHOU, YANGYANG LU, WEIWEI ZHU, RUI MIN, *Electro-optic directed logic circuit based on microring resonators for XOR/XNOR operations*, Optics Express **20**(11), 2012, pp. 11605–11614.

[36] RAKSHIT J.K., ROY J.N., CHATTOPADHYAY T., *All-optical XOR/XNOR logic gate using micro-ring resonator*, 5th International Conference on Computers and Devices for Communication (CODEC), Kolkata, India, December 17–19, 2012, pp. 1–4.

[37] OLSSON B-E., BLUMENTHAL D.J., *WDM to OTDM multiplexing using an ultrafast all-optical wavelength converter*, IEEE Photonics Technology Letters **13**(9), 2001, pp. 1005–1007.

[38] HAMILTON S.A., ROBINSON B.S., MURPHY T.E., SAVAGE S.J., IPPEN E.P., *100 Gb/s optical time-division multiplexed networks*, Journal of Lightwave Technology **20**(12), 2002, pp. 2086–2100.

[39] ROY J.N., MAITI A.K., MUKHOPADHYAY S., *Designing of an all-optical time division multiplexing scheme with the help of nonlinear material based tree-net architecture*, Chinese Optics Letters **4**(8), 2006, pp. 483–486.

[40] ZHAN-QIANG HUI, JIAN-GUO ZHANG, *Design of polarity-preserved or polarity-inverted wavelength converters using cross-phase modulation in a highly nonlinear photonic crystal fiber with flat dispersion*, Journal of Optics **14**(6), 2012, article 065402.

[41] LIN S., ISHIKAWA Y., WADA K., *Demonstration of optical computing logics based on binary decision diagram*, Optics Express **20**(2), 2012, pp. 1378–1384.

[42] VAN V., IBRAHIM T.A., ABSIL P.P., JOHNSON F.G., GROVER R., HO P.-T., *Optical signal processing using nonlinear semiconductor microring resonators*, IEEE Journal of Selected Topics in Quantum Electronics **8**(3), 2002, pp. 705–713.

[43] RABUS D.G., HAMACHER M., *MMI-coupled ring resonators in GaInAsP–InP*, IEEE Photonics Technology Letters **13**(8), 2001, pp. 812–814.

[44] RABUS D.G., HAMACHER M., HEIDRICH H., *Resonance frequency tuning of a double ring resonator in GaInAsP/InP: experiment and simulation*, Japanese Journal of Applied Physics, Part 1, **41**(2B), 2002, pp. 1186–1189.

[45] CHUNPANG P., PIPHITHIRANKARN P., YUPAPIN P.P., *An investigation of quantum–chaotic signals generation using a fiber ring resonator and an add/drop multiplexer*, Optik – International Journal for Light and Electron Optics **121**(8), 2010, pp. 765–769.

[46] RAKSHIT J.K., CHATTOPADHYAY T., ROY J.N., *Design of ring resonator based all optical switch for logic and arithmetic operations – a theoretical study*, Optik – International Journal for Light and Electron Optics **124**(23), 2013, pp. 6048–6057.

[47] THONGMEE S., YUPAPIN P.P., *All optical half adder/subtractor using dark-bright soliton conversion control*, Procedia Engineering **8**, 2011, pp. 217–222.

[48] PHONGSANAM P., TEEKA C., JOMTARAK R., MITATHA S., YUPAPIN P.P., *All-optical logic AND and OR gates generated by dark–bright soliton conversion*, Optik – International Journal for Light and Electron Optics **124**(5), 2013, pp. 406–410.

[49] SAEUNG P., YUPAPIN P.P., *Generalized analysis of multiple ring resonator filters: modeling by using graphical approach*, Optik – International Journal for Light and Electron Optics **119**(10), 2008, pp. 465–472.

[50] ZOIROS K.E., PAPADOPOULOS G., HOUBAVLIS T., KANELLOS G.T., *Theoretical analysis and performance investigation of ultrafast all-optical Boolean XOR gate with semiconductor optical amplifier-assisted Sagnac interferometer*, Optics Communications **258**(2), 2006, pp. 114–134.

[51] HOUBAVLIS T., ZOIROS K.E., KANELLOS G., TSEKREKOS C., *Performance analysis of ultrafast all-optical Boolean XOR gate using semiconductor optical amplifier-based Mach–Zehnder interferometer*, Optics Communications **232**(1–6), 2004, pp. 179–199.

[52] TARAPHDAR C., CHATTOPADHYAY T., ROY J.N., *Mach–Zehnder interferometer-based all-optical reversible logic gate*, Optics and Laser Technology **42**(2), 2010, pp. 249–259.

[53] VARDAKAS J.S., ZOIROS K.E., *Performance investigation of all-optical clock recovery circuit based on Fabry–Pérot filter and semiconductor optical amplifier assisted Sagnac switch*, Optical Engineering **46**(8), 2007, article 085005.

Received May 28, 2013
in revised form September 2, 2013